INVESTIGATION OF INFLUENCE OF CAVITATION ON FLOW RATE OF SPOOL NOTCH USING COMPUTATIONAL FLUID DYNAMICS

Koji SHIWAKU and Kento KUMAGAI

Advanced Development Center
Hitachi Construction Machinery Co., Ltd.
650 Kandatsu, Tsuchiura, Ibaraki, 300-0013 Japan
(E-mail: k.shiwaku.ur@hitachi-kenki.com)

Abstract. The notch is used to adjust the spool valve that performs delicate flow control operations in hydraulic systems for construction machinery, and notch flow control characteristics are important for overall valve performance. However, these flow characteristics change under the influence of cavitation. Therefore, understanding of the correlation between cavitation and flow is important for spool valve design. The influence of cavitation on notch flow characteristics and causes of cavitation in hydraulic systems are investigated using visualization experiments and computational fluid dynamics (CFD) simulations. The flow rate of the notch in the experiments varied depending on the presence or absence of cavitation, even if the pressure difference was the same, and the experimental results and CFD results show good agreement. The CFD results also showed that the flow path's cross-sectional area inside the notch decreased because of the occurrence of cavitation and this caused the notch flow characteristics to fluctuate.

Keywords: Cavitation, Spool Valve, Hydraulics, CFD, Flow Rate

INTRODUCTION

In construction machinery composed of a variety of hydraulic devices, the spool valve is one of the most important components, and is used to control the flow rate that is sent to the actuator of the construction machinery. Operability is one of the most important performance measures for construction machinery, and high accuracy is thus required for the flow control that determines the operability of the actuator. To realize high accuracy flow control, fine adjustment of the spool valve's opening area using the notch is necessary. However, in systems that require control of both high pressure and large flow rates, like the hydraulic systems of construction machinery, cavitation [1] is known to occur in the throttle section of the spool valve. Additionally, this cavitation is known to affect the flow characteristics of the spool valve [2]. Therefore, cavitation represents a serious disturbance to the notch, which requires delicate flow control [3]. Therefore, the effects of cavitation on the flow characteristics of the spool valve, including its effects on the notch, represent an important consideration in spool valve design. However, because it is technically difficult to measure the complex dynamics of cavitation when it occurs in a flow field that involves high flow velocities and high pressure inside hydraulic components, it is also difficult to investigate the influence of cavitation on the flow characteristics of the spool notch using an experimental approach. Fortunately, thanks to the rapid development of computational fluid dynamics (CFD) simulation technology in recent years, detailed analysis of the flow fields inside hydraulic components that remain difficult to measure has become possible using CFD simulations. Several reports on cavitation in the flow fields of spool valves have been reported, and the pressure distribution [4] and the behavior of the cavitation bubbles [5] of the flow field have been investigated. However, few detailed investigations of the correlation between the spool valve flow characteristics and cavitation have been performed using CFD. In this paper, the influence of cavitation on the flow characteristics of the notch and the causes of cavitation in the hydraulic system are investigated using visualization experiments and CFD simulations.

METHOD AND CONDITIONS

Experiment

The configuration of the experimental system is as shown in Figure 1, and the spool valve that was tested is shown in Figure 2. The experimental system consists of: a variable displacement-type axial piston pump (1): the

spool valve under test (2): an oil tank (3); a pressure control valve for upstream pressure adjustment, installed upstream of the spool valve (4); a pressure control valve for downstream pressure adjustment, installed downstream of the spool valve (5); and an oil cooler (6). The spool valve under test (2) consists of the upstream valve block, the downstream valve block, the spool, the handle for spool displacement adjustment, and the feed screw shaft that connects the handle with the spool. The downstream valve block is made from acrylic resin for measurements using a high-speed camera. In the experiments, the downstream pressure P_d is set at 0.2 MPa (gauge) and 1.5 MPa (gauge), where P_d = 0.2 MPa represents a condition with cavitation in the downstream section and P_d = 1.5 MPa represents a condition without cavitation in the downstream section. Additionally, the differential pressure of the spool valve under test, denoted by ΔP, is set at 2±0.05 MPa using the upstream and downstream pressure control valves, and is constant under all experimental conditions. The liquid used is a mineral-oil-based hydraulic fluid with an International Organization for Standardization (ISO) viscosity grade of 46 (kinematic viscosities of 45.47×10^{-6} m^2/s at 40°C and oil density of 842 kg/m^3), and the oil temperature T is set at 50±2°C by the oil cooler. The volumetric flow rate of the hydraulic oil that passed through the tested spool valve Q was measured using a gear-type flowmeter that was installed on the upstream side, which was not affected by cavitation. The spool displacement x is set in the range from 0 to 4 mm using the handle and the feed screw. The notch geometry is shown in Figure 3. The notch is a U-groove type, with depth d of 1 mm, diameter D of 3 mm and length l of 5.5 mm. The high-speed video camera shooting conditions were set at a frame rate of 3382 fps and a shutter speed of 1/250000 s, and the images were recorded using a monochrome lens. The measured data were recorded on a personal computer (PC).

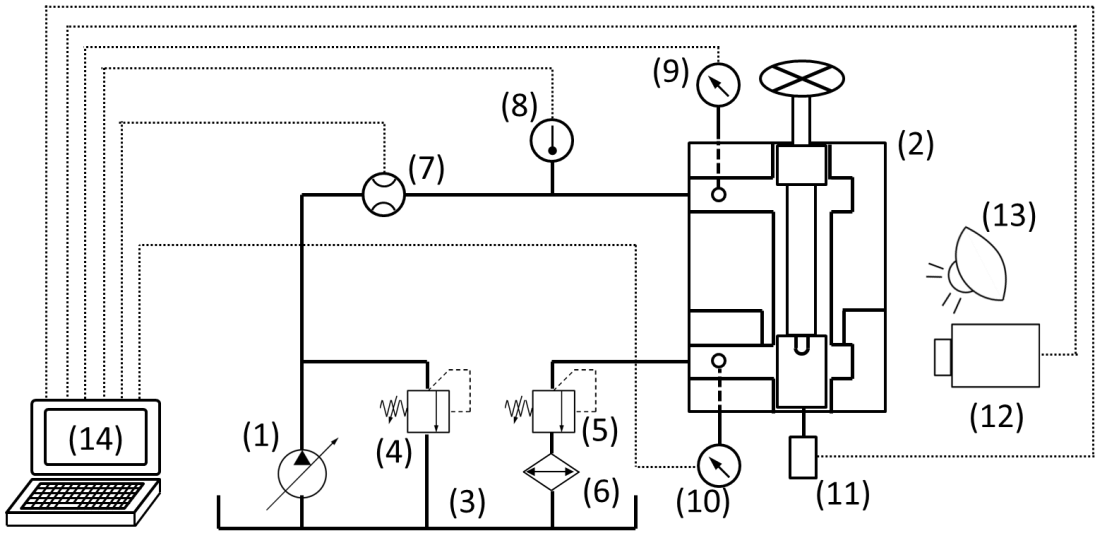

(1) Pump; (2) spool valve under test; (3) oil tank; (4) pressure control valve (upstream); (5) pressure control valve (downstream); (6) oil cooler; (7) flowmeter; (8) thermometer; (9) pressure transducer (upstream); (10) pressure transducer (downstream); (11) stroke sensor; (12) high-speed video camera and digital camera; (13) halogen light; (14) personal computer (PC) for data logging.

FIGURE 1. Experimental system.

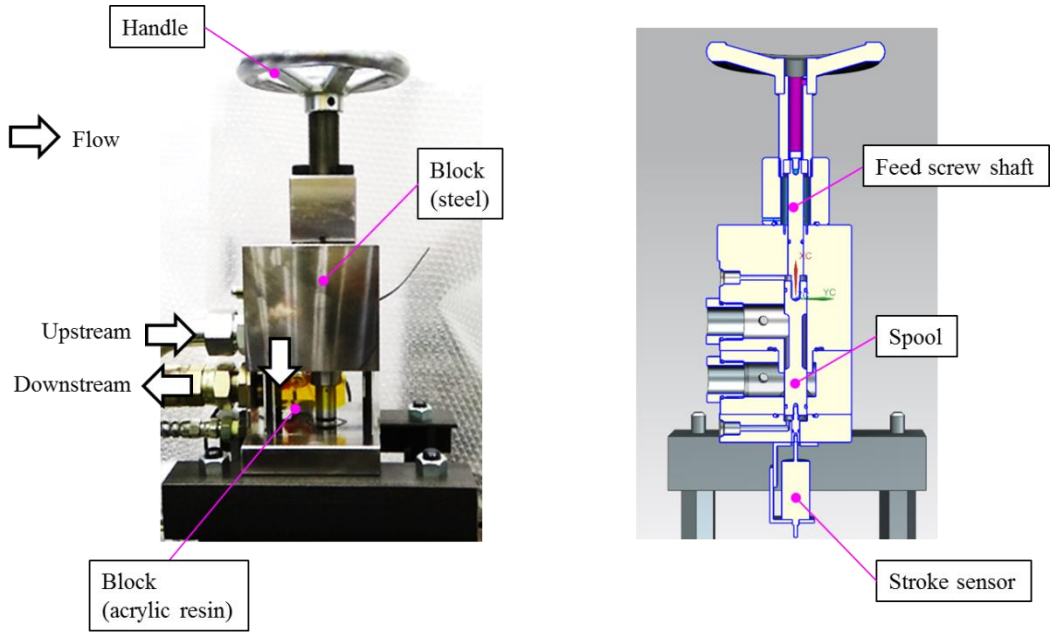

FIGURE 2. Spool valve to be tested.

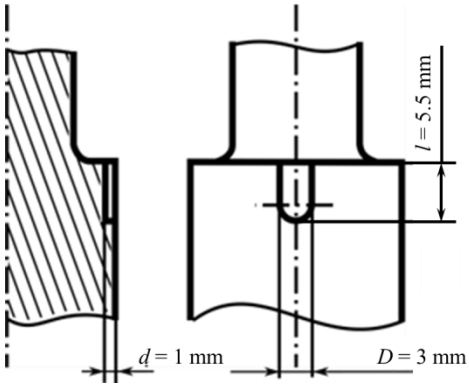

FIGURE 3. Geometry of U-groove notch.

Simulation

The simulation model that was created using STAR-CCM+ Ver.11.02.0110 software (CD-adapco) is shown in Figure 4. The shape of the flow path is the same as that of the spool valve under test in the experiments. The locations of the inlet and outlet boundaries were set at the same locations as those of the pressure transducer on the experimental device, with both locations being 30 mm away from the center axis of the spool. The downstream pressure P_d was set at 0.301325 MPa (absolute) and 1.601325 MPa (absolute), and the differential pressure ΔP was set at 2 MPa. The other conditions were set at the same values as the experimental conditions. Two mesh types were used: a polyhedral mesh and a prism layer mesh. The element sizes of the polyhedral mesh were 0.05 mm at the notch and 0.3–3 mm at the other parts. The total number of wall boundary layers comprised 10 prism layers, and the height was set at 0.05 mm. The turbulence model used was a shear stress transport (SST) k-ω model [6]. The Rayleigh-Plesset formula [7] that is used as the basis for the cavitation model is shown in Eq. (1):

$$R\frac{d^2R}{dt^2}+\frac{3}{2}\left(\frac{dR}{dt}\right)^2=\frac{P_B-P_\infty}{\rho_L}-\frac{2\sigma}{P_lR}-4\frac{u_l}{P_lR}\frac{dR}{dt} \quad (1)$$

In this simulation, the simplified Rayleigh-Plesset formula of Eq. (2), which excludes the terms for fluid inertia, surface tension, and viscosity from Eq. (1), was used:

$$\left(\frac{dR}{dt}\right)^2 = \frac{2}{3}\frac{P_B - P_\infty}{\rho_L} \tag{2}$$

Here, R is the radius of a cavitation bubble, P_B is the pressure within the cavitation bubble, P_∞ is the external pressure at an infinite distance from the cavitation bubble, and ρ_L is the density of the surrounding liquid. In the simulations, P_B was set as the air separated pressure of the oil of 25700 Pa, because the saturated vapor pressure of the oil is much lower. Based on the experimental data, the other oil parameters were set, with a bulk modulus K of 1.6 GPa, an initial bubble radius R_0 of 1×10^{-7} m, and a bubble density n_0 of 1×10^{7} number/m^3. The simulation model was solved using implicit unsteady solver, and a time step of Δt = 10 μs. Δt was set based on the bubble velocity acquired using the data from the high-speed camera.

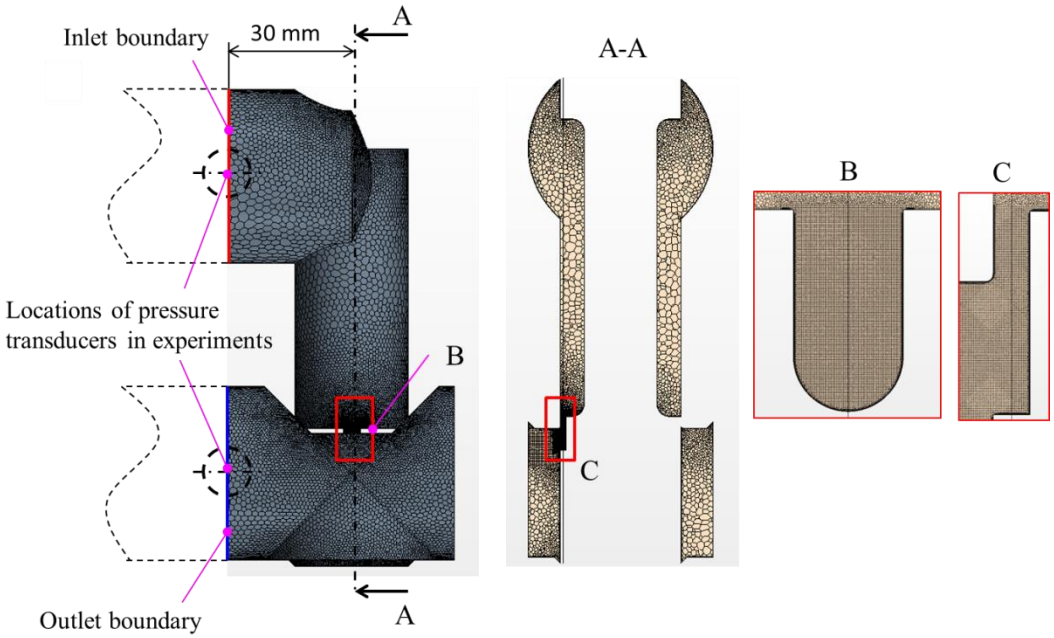

FIGURE 4. Simulation model.

RESULTS AND DISCUSSION

Flow Characteristics of Spool Notch

The spool notch flow characteristics obtained from the experiments are shown in Figure 5. Figure 5(a) shows the flow rate versus the spool displacement, where the horizontal axis shows spool displacement x and the vertical axis shows the average flow rate Q_{ave}. Figure 5(b) shows an enlarged section of the results under the conditions where the difference between the results at P_d = 0.2 MPa and 1.5 MPa was large. Q_{ave} represents a time average of the flow rate Q that is used to reduce data noise from the flow rate waveform that includes time dispersion due to disturbances such as pump pulsation or the measurement error of the measuring device, as shown in Figure 5(d). Figure 5(c) shows the correspondence between the notch shape and the displacement shown in Figure 5(a). Under the conditions at an arbitrary point in Figure 5(a), the notch area on the left side that is separated by the perpendicular line passing through the arbitrary point represents the opening portion.

In Figure 5(a), Q_{ave} increases rapidly with increasing spool displacement at $x < 1.5$ mm and becomes relatively stable at $x \geq 1.5$ mm. This tendency is similar to the characteristic of the theoretical opening area with respect to displacement of the U-groove notch, where the theoretical opening area increases with increasing spool displacement at $x < 1.5$ mm and becomes constant at $x \geq 1.5$ mm. However, as shown in Figure 5(b), there was a difference in the values of Q_{ave} between the conditions of P_d = 0.2 MPa and 1.5 MPa at $x \geq 1.5$ mm. This difference indicates that the cavitation is the cause of the difference in flow rate, even though the theoretical opening area and the differential pressure are both the same.

Figure 6 shows the state of cavitation of the notch portion as photographed using the high-speed video camera under the conditions of P_d = 0.2 MPa and 1.5 MPa for each value of spool displacement x. The photographs confirm that cavitation bubbles are present when P_d = 0.2 MPa and are absent when P_d = 1.5 MPa at any spool

displacement. Furthermore, it is noted that the cavitation bubbles are present not only downstream of the notch but also inside the notch. These results show that there are cases where the flow rate under the condition that the cavitation bubbles are present decreases when compared with the condition where the cavitation bubbles are absent; it can then be inferred that the cause of this behavior is strongly related to the cavitation that occurred in the notch portion.

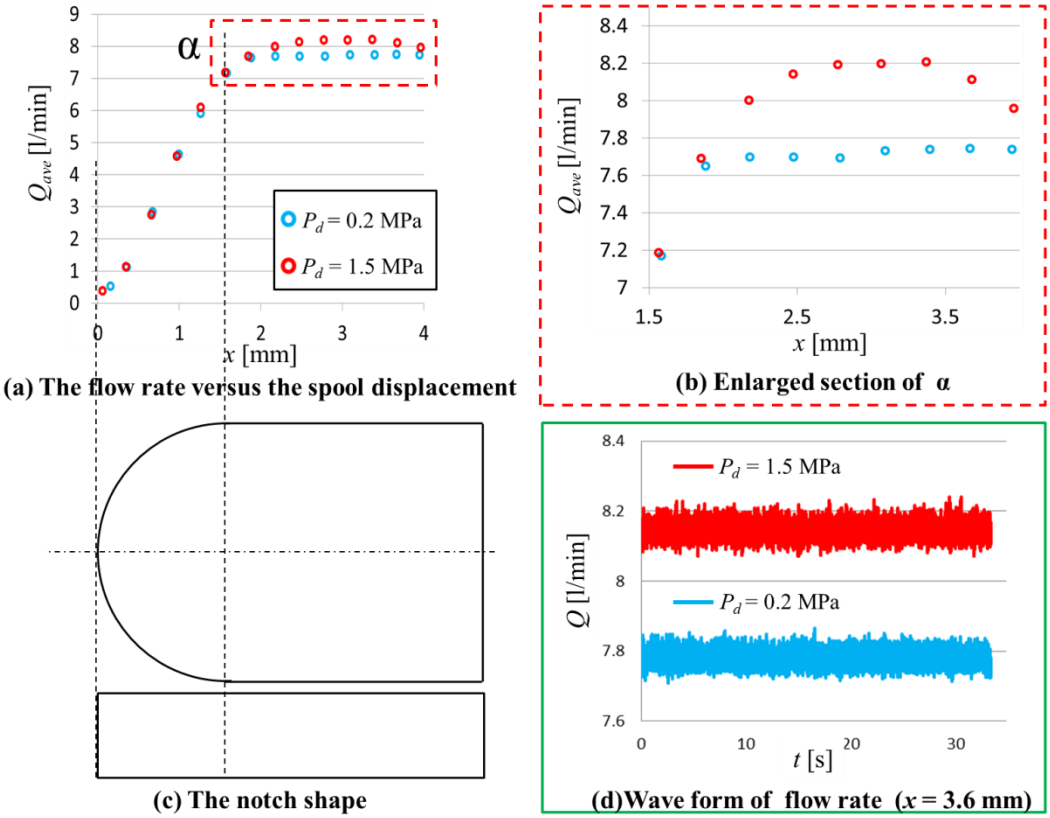

FIGURE 5. Flow characteristics of notch in experiments.

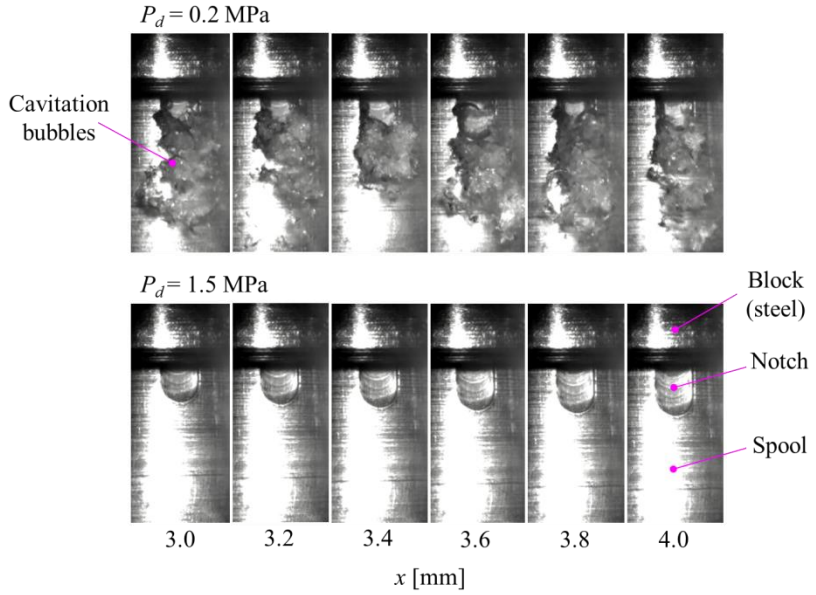

FIGURE 6. State of cavitation.

Influence of cavitation

A comparison of the spool notch characteristics obtained from the experimental results and the simulation results is shown in Figure 7. Figure 7(b) shows an enlarged section of the results under the conditions where the difference between the results for P_d = 0.2 MPa and 1.5 MPa was large. The horizontal axis represents the spool displacement x and the vertical axis is the averaged flow rate Q_{ave}, while the circular makers indicate the experimental data and the square markers indicate the simulation data. The simulation results showed flow characteristics that were similar to those of the experimental results. In particular, under the condition where $x \geq$ 1.5 mm, the difference in flow between P_d = 0.2 MPa and 1.5 MPa is clearly observed even in the simulation results. From these results, it was clear that the increase in flow loss occurs because of the effects of cavitation in the flow field of the spool notch. However, because the flow rate drop due to the effects of cavitation occurs under partial displacement rather than full displacement conditions, it is not possible to explain the phenomenon based on the occurrence of cavitation caused by low downstream pressure alone. Therefore, the increased flow losses are assumed to be due to cavitation and other factors acting in combination.

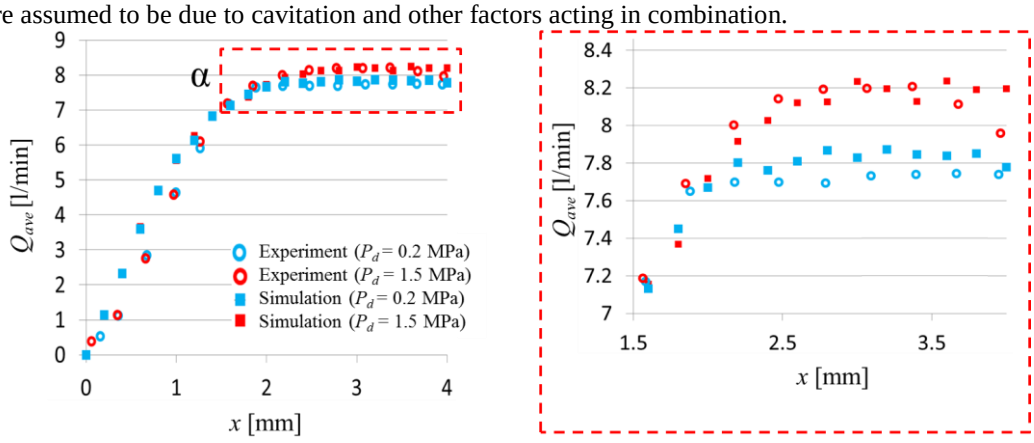

FIGURE 7. Comparison of experimental results with simulation results.

Status of Cavitation in the Notch

The distribution of the cavitation bubbles at x = 3.6 mm is shown in Figure 8. The upper row shows photographs of the cavitation bubbles in the notch section taken using the high-speed camera, and the lower row shows images of the volume fraction of the gas that were acquired from the CFD simulation results. The experimental results show that the cavitation bubbles are distributed inside and behind the notches, and the simulation results show similar distributions. In addition, these results confirm that the cavitation bubbles continue to occur relatively stably based on the behavior of the cavitation bubbles when arranged in chronological order. It is not possible to compare the numbers of bubbles from the images obtained using the high-speed video camera quantitatively, but the behavior and the distributions of the cavitation bubbles shown in the experimental results and simulation results can be said to agree qualitatively with each other. The simulation results show that cavitation has already occurred at the inlet of the notch, although this could not be visualized in the experimental images, and the cavitation bubbles are also present inside the notch.

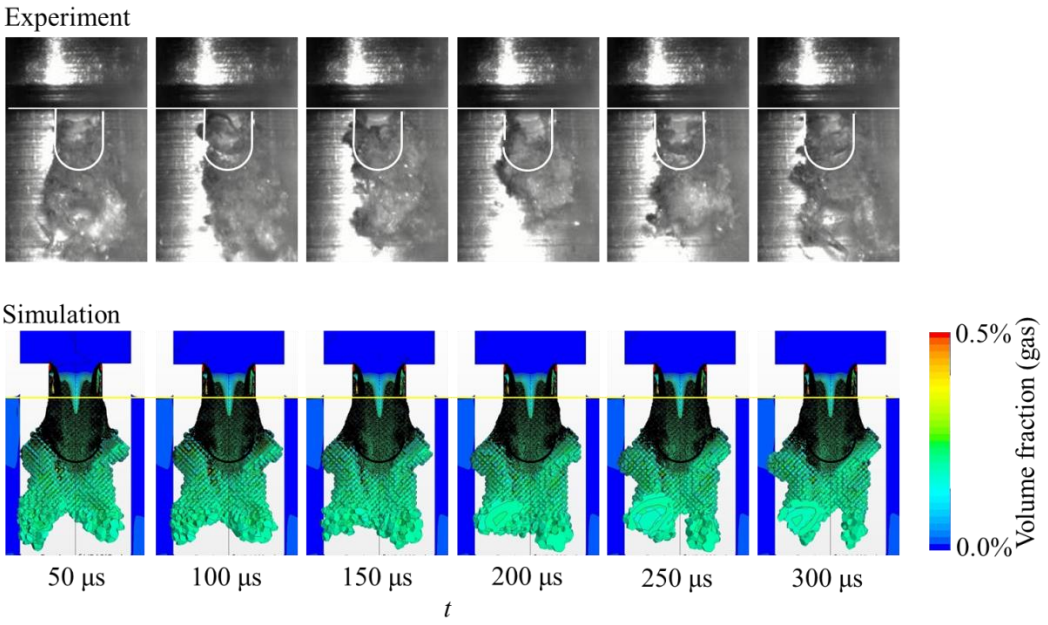

FIGURE 8. Distributions of cavitation in notch portion.

The influence of the distribution of the cavitation bubbles inside the notch will now be discussed in detail. A comparison of the magnitude of the flow velocities from the simulation results at P_d = 0.2 MPa and P_d = 1.5 MPa is shown in Figure 9. Figure 9(a) shows the position of the cross-sectional area at which the flow velocity distribution x_{cross} was acquired at x = 3.6 mm. Figure 9(b) shows the distributions of the velocity magnitude V_{mag} at the cross-sections at x_{cross} = 0.8, 1.6, 2.4, 3.2, 4.0 mm, where the pink contours indicate the distributions of the cavitation bubbles. In addition, the black line shows the distribution at which V_{mag} = 30 m/s, and the part where V_{mag} > 30 m/s is defined as the high flow velocity section based on the black line in this work. V_{mag} was low in the vicinity of the wall inside the notch while the flow velocity was high in the central part of the notch, and the flow distributions showed similar trends under both conditions. However, the distribution of the cavitation bubbles can be confirmed on the bottom or the side of the interior of the notch at P_d = 0.2 MPa. Additionally, when the distribution areas of the high flow velocity sections are compared in detail, it is observed that the distribution areas of the high flow velocity section were reduced at P_d = 0.2 MPa. Because V_{mag} of the high flow velocity part is approximately the same under both conditions, these results mean that the cross-sectional area of the flow passage decreases because of the occurrence of cavitation. From these results, the flow path area was found to decrease because of the cavitation generated inside the notch under the condition where the flow rate decreased with the occurrence of cavitation. Additionally, it can be concluded that this decrease in the flow area is a physical cause of the increased flow loss that accompanies cavitation.

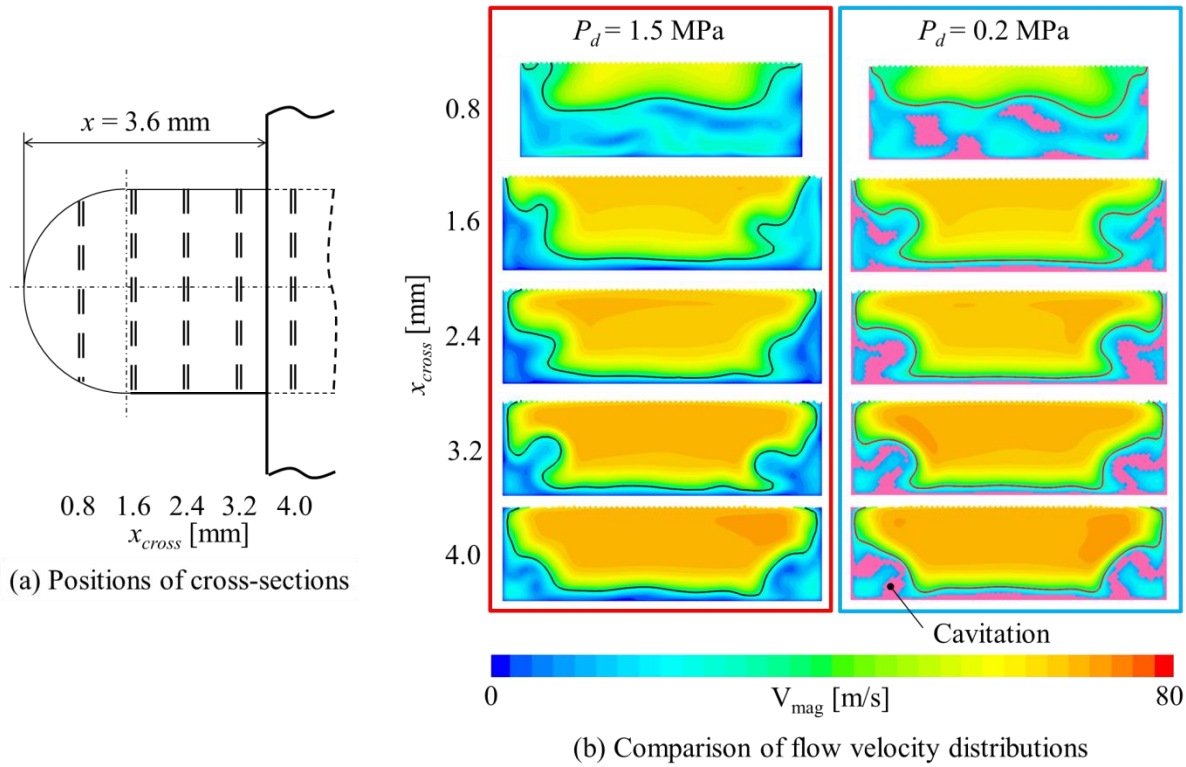

FIGURE 9. Comparison of cross-sectional areas of flow inside notch.

CONCLUSIONS

In this paper, the effects of cavitation on the flow characteristics of the notch in a spool valve and the cause of this cavitation in the hydraulic system are investigated using a combination of visualization experiments and CFD simulations. The following results were obtained. 1) In the experiments, the flow rate decreased under certain spool displacement conditions in the flow field under which cavitation occurs behind and inside the notch section. 2) A flow reduction phenomenon was also shown in the CFD simulation results when using the cavitation calculation model. 3) An examination of the flow field inside the notch via CFD simulation revealed that the cavitation that is generated inside the notch reduces the flow path area inside the notch, which then causes the reduction in the flow rate. These results are helpful in explaining the fluctuations in the spool flow characteristics in a flow field with cavitation and in the design of the spool valve.

REFERENCES

1. KNAPP, R. T., DALLY, J. W., HAMMITT, F. G., Cavitation, McGraw Hill, New York, 1969, pp. 1–20.
2. MCCLOY D., BECK, A., Some Cavitation Effects in Spool Valve Orifices, Proceedings of the Institution of Mechanical Engineers, Vol. 182, No. 8, 1967–68, pp.163–174.
3. LU, L., et al., Cavitating Flow in Non-Circular Opening Spool Valves with U-Grooves, Proceedings of the Institution of Mechanical Engineers, Part C, Journal of Mechanical Engineering Science, Vol. 223, No. 10, 2009, pp. 2297–2307.
4. FU, X., JI, H., RYU, S., Investigation into Pressure Distribution of Spool Valve with Notches, Proceedings of the 6th JFPS International Symposium on Fluid Power TSUKUBA 2005, 2005, No. 3A1-3, pp. 635–639.
5. SCHÜMICHEN, M., RÜDIGER F., FRÖHLICH, J., WEBER, J., Simulation of the Cavitating Flow in a Model Oil Hydraulic Spool Valve using Different Model Approaches, 10th International Fluid Power Conference (10. IFK), 2016, Vol. 1, pp. 321–332.
6. MENTER, F. R., Two-Equation Eddy-Viscosity Turbulence Models for Engineering Applications, AIAA Journal, Vol. 32, No. 8, 1994, pp. 1598–1605.
7. BRENNEN C. E., Cavitation and Bubble Dynamics, Oxford University Press, New York, 1995, pp. 48–53.

